Subwords as Skills: Tokenization for Sparse-Reward Reinforcement Learning

David Yunis* **Justin Jung†** **Falcon Dai*** **Matthew Walter***
*Toyota Technical Institute of Chicago, {dyunis, fdai, mwalter}@ttic.edu
†University of Chicago, jsjung@uchicago.edu

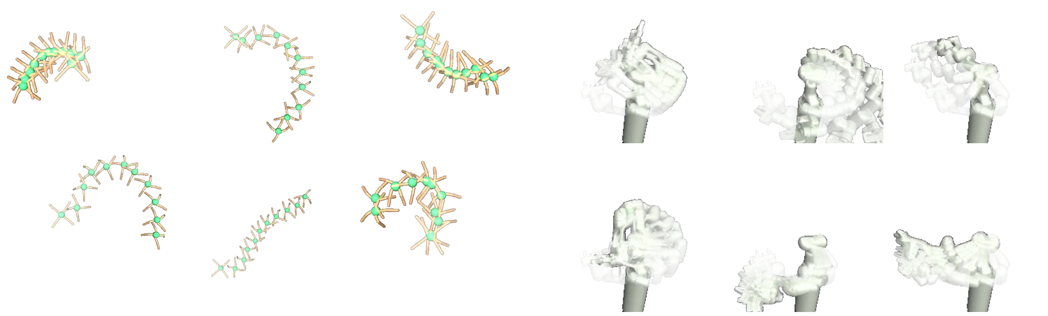

(a) AntMaze (b) Kitchen

Figure 1: A sample of some "skills" that our method identifies for the (a) AntMaze and (b) Kitchen environments, where the transparency is higher (color is paler) for poses earlier in the trajectory. For more discussion see Appendix B.

Abstract

Exploration in sparse-reward reinforcement learning (RL) is difficult due to the need for long, coordinated sequences of actions in order to achieve any reward. Moreover, in continuous action spaces there are an infinite number of possible actions, which only increases the difficulty of exploration. One class of methods designed to address these issues forms temporally extended actions, often called skills, from interaction data collected in the same domain, and optimizes a policy on top of this new action space. Such methods require a lengthy pretraining phase in order to form the skills before reinforcement learning can begin. Given prior evidence that the full range of the continuous action space is not required in such tasks, we propose a novel approach to skill-generation with two components. First we discretize the action space through clustering, and second we leverage a tokenization technique borrowed from natural language processing to generate temporally extended actions. Using this as an action-space for RL outperforms comparable skill-based approaches in several challenging sparse-reward domains, and requires orders-of-magnitude less computation.

1 Introduction

Reinforcement learning (RL), the learning paradigm that allows an agent to interact with an environment and collect its own data, is a promising approach to learning in many domains where high-quality data collection is too financially expensive or otherwise intractable. Though it began with dynamic programming in tabular settings, the recent use of neural networks as function approximators

NeurIPS 2023 Workshop on Generalization in Planning (GenPlan 2023).

has led to great success on many challenging learning tasks [Mnih et al., 2013, Silver et al., 2017, Gu et al., 2017]. These successful tasks tend to have some particular properties. In some cases, it is simple to define a reward function that yields reward at every step of interaction (the “dense” reward setting), like directional velocity of a robot learning to walk [Haarnoja et al., 2018a]. In other cases, the environment dynamics are known, as in the case of Chess or Go [Silver et al., 2017]. However, for many natural tasks like teaching a robot to make an omelet, it is much more straightforward to tell when the task is completed without knowing how to automatically supervise each individual step, how to model the environment dynamics. Learning in these “sparse” reward settings, where reward is only obtained extremely infrequently (e.g., at the end of successful episodes) is notoriously difficult. In order for a learning agent to improve its policy, the agent needs to explore its environment for long periods of time, often in a coordinated fashion, until it finds any reward.

One class of solutions to this problem involves including additional task-agnostic dense rewards as bonuses that encourage agents to explore the state space [Pathak et al., 2017, Burda et al., 2018b]. Another class of solutions to the exploration issue is to jumpstart the function approximator to be used in reinforcement learning by training it on some pretext task [Yarats et al., 2021, Liu and Abbeel, 2021], which works well when the training and downstream domains are well aligned. A third class of methods aims to create temporally extended actions, or “skills”, from interactions or data. A particular subclass of methods learns skills that are conditioned on the observations [Singh et al., 2020, Pertsch et al., 2021, Ajay et al., 2020, Sharma et al., 2019, Eysenbach et al., 2018, Park et al., 2022, 2023], which means that the deployment scenario needs to match the data. Others relax this assumption [Lynch et al., 2020, Pertsch et al., 2021, Bagatella et al., 2022] so that such skills can easily be transferred to some new domain as long as the action space remains the same. This has the potential to speed up exploration in new tasks for which it is not easy to collect data a priori (i.e., few-shot), which can lead to faster task adaptation. However, these recent efforts in skill learning all require lengthy pretraining phases due to their reliance on neural networks in order to learn the skills. Inspired by the recent cross-pollination of natural language processing (NLP) techniques in offline RL [Chen et al., 2021, Janner et al., 2021, Shafiullah et al., 2022], we take a different approach.

Like the long-range coordination required for exploration in sparse-reward RL, language models must model long range dependencies between discrete tokens. Character inputs leads to extremely long sequences, and requires language models to both spell correctly and model inter-word relations. On the other hand, word-level input results in the model poorly capturing certain rare and unseen words. The solution is to create “subword” tokens somewhere in between individual characters and words that can express any text [Gage, 1994, Sennrich et al., 2015, Provilkov et al., 2020, Kudo, 2018, Schuster and Nakajima, 2012, He et al., 2020].

In the spirit of this development in language modeling, we propose a tokenization method for learning skills. Following prior work [Dadashi et al., 2022, Shafiullah et al., 2022], we discretize the action space and use a modified byte-pair encoding (BPE) scheme [Gage, 1994, Sennrich et al., 2015] to obtain temporally extended actions. Then, we use this as the action-space for RL. As we demonstrate, such a method benefits from extremely fast skill-generation (minutes v.s. hours for neural network-based methods), significantly faster rollouts and training due to open-loop subword execution that does not require an additional neural network, interpretability of a finite set of skills, and strong results in several sparse-reward domains.

2 Related Work

Exploration in RL: Exploration is a fundamental problem in RL, particularly when reward is sparse. A common approach to encouraging exploratory behavior is to augment the (sparse) environment reward with a dense bonus term that biases toward exploration. This includes the use of state visitation counts [Poupart et al., 2006, Lopes et al., 2012, Bellemare et al., 2016] and state entropy objectives [Mohamed and Jimenez Rezende, 2015, Hazan et al., 2019, Lee et al., 2019, Pitis et al., 2020, Liu and Abbeel, 2021, Yarats et al., 2021] that incentivize the agent to reach “novel” states. Related, “curiosity”-based exploration bonuses encourage the agent to take actions in states where the effect is difficult to predict using a learned forward [Schmidhuber, 1991, Chentanez et al., 2004, Stadie et al., 2015, Pathak et al., 2017, Achiam and Sastry, 2017, Burda et al., 2018a] or inverse [Haber et al., 2018] dynamics model. Burda et al. [2018b] propose a random network distillation exploration bonus based upon the error in observation features predicted by a randomly initialized neural network.

Temporally Extended Actions and Hierarchical RL: Another long line of work explores temporally extended actions due to the potential for such abstractions to improve learning efficiency. These advantages are particularly pronounced for difficult learning problems including sparse reward tasks, which is the focus of our work. In particular, action abstractions enable more effective exploration [Nachum et al., 2018] and simplify the credit assignment problem. Hierarchical reinforcement learning (HRL) [Dayan and Hinton, 1992, Kaelbling, 1993, Sutton, 1995, Boutilier et al., 1997, Parr and Russell, 1997, Parr, 1998, Sutton et al., 1999, Dietterich, 2000, Barto and Mahadevan, 2003, Kulkarni et al., 2016, Bacon et al., 2017, Vezhnevets et al., 2017] considers the problem of learning policies with successively higher levels of abstraction (typically two), whereby the lowest level considers actions directly applied in the environment while the higher levels reason over temporally extended transitions. A classic example of action abstractions is the options framework [Sutton et al., 1999] , which provides a standardization of HRL in which an option is a terminating sub-policy that maps states (or observations) to low-level actions. Options are often either prescribed as predefined low-level controllers or learned via subgoals or explicit intermediate rewards [Dayan and Hinton, 1992, Dietterich, 2000, Sutton et al., 1999]. Some simple instantiations of options include repeated actions [Sharma et al., 2017] and self-avoiding random walks [Amin et al., 2020]. Konidaris and Barto [2009] learn a two-level hierarchy by incrementally chaining options ("skills") backwards from the goal state to the start state. Nachum et al. [2018] propose a hierarchical learning algorithm (HIRO) that learns in an off-policy fashion and, in turn, is more sample-efficient than typical HRL algorithms, which learn on-policy. Achieving these sample efficiency gains requires addressing the instability typical of off-policy learning, which is complicated by the non-stationarity that comes with jointly learning low- and high-level policies. Levy et al. [2017] use different forms of hindsight [Andrychowicz et al., 2017] to address similar instability issues that arise when learning policies at multiple levels in parallel.

Skill Learning from Demonstrations: In addition to the methods mentioned above in the context of HRL, there is an existing body of work that seeks to discover extended actions prior to their use in online RL, often called "skills". Many methods have been developed for skill discovery from interaction [Daniel et al., 2012, Gregor et al., 2016, Eysenbach et al., 2018, Warde-Farley et al., 2018, Park et al., 2022, 2023]. Most related to our setting is a line of work that explores extended action discovery from demonstration data [Lynch et al., 2020, Ajay et al., 2020, Singh et al., 2020, Pertsch et al., 2021, Bagatella et al., 2022]. As an example, Lynch et al. [2020] learn a VAE on chunks of action sequences in order to generate a temporally extended action by sampling a single vector. Ajay et al. [2020] follow a similar approach, but use flow models on top of entire trajectories, and only rollout a partial trajectory at inference time. Some of these methods [Ajay et al., 2020, Singh et al., 2020, Pertsch et al., 2021] condition on the observations when learning skills, which leads to more efficient exploration, but such conditioning means that any skill that is learned will need to be deployed in the same environment as the one in which the data was collected, resulting in poor domain transfer performance [Bagatella et al., 2022]. Others [Lynch et al., 2020, Bagatella et al., 2022] simply condition on actions, which means that the skills can be reused in any domain that shares the same action space. In an effort to learn more generalizable skills, we follow this latter example. There is also a related prior work that applies grammar-learning to online RL [Lange and Faisal, 2019], but such a method learns an ever-growing number of longer actions, which poses significant issues in the sparse-reward setting, as we discuss later.

3 Method

Similar to prior work [Lynch et al., 2020, Ajay et al., 2020, Singh et al., 2020, Pertsch et al., 2021, Bagatella et al., 2022], we extract skills from demonstration data, more formally a dataset of N trajectories with lengths $\{n_i\}_{i \in N}$ that involve the same action space as our downstream task

$$\mathcal{D} = \left\{ (o_{ij}, a_{ij})_i | i \in \mathbb{N} \cap [0, N),\ j \in \mathbb{N} \cap [0, n_i),\ o_{ij} \in \mathbb{R}^{d_{\text{obs}}},\ a_{ij} \in \mathbb{R}^{d_{\text{act}}} \right\},$$

where a_{ij} and o_{ij} denote actions and observations, respectively. After extracting skills from this dataset, we use these skills as a new action space for reinforcement learning on some downstream task. Crucially, our skills are unconditional so do not have any information as to when they should be used in the downstream task. In following sections we detail our exact method.

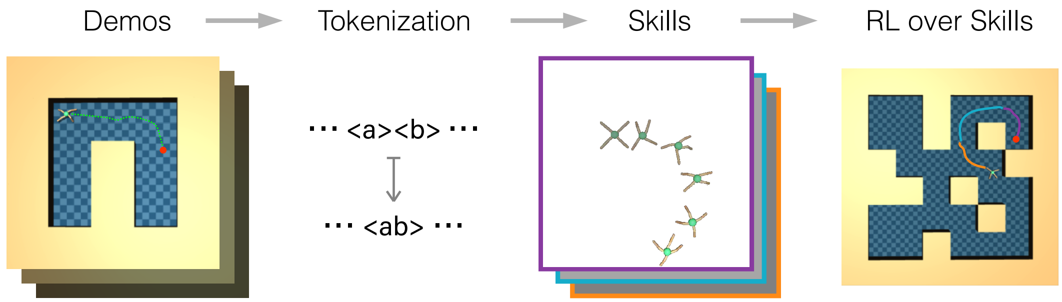

Figure 2: Abstract representation of our method. Given demonstrations in the same action space as our downstream task, we discretize the actions and apply tokenization techniques to recover “subwords” that form a vocabulary of skills. We then train a policy on top of these skills for some new task. We only require a common action space between demonstrations and downstream task.

3.1 Byte-Pair Encoding

Byte-pair encoding (BPE) was first proposed as a simple method to compress files [Gage, 1994], but it has recently been used to construct vocabularies for NLP tasks in between the resolution of characters and whole-words [Sennrich et al., 2015]. With character vocabularies, the vocabulary is small, but the sequence lengths are large. Such long sequences are extremely burdensome to process, especially for the current generation of Transformers. In addition, making predictions at the character level imposes a more difficult task on the language model: it needs to spell everything correctly, or make a long-coordinated set of predictions, not unlike the requirement on action sequences for sparse-reward exploration. Whole-word vocabularies shorten the sequence lengths and make the prediction task easier, but if a word is rare in the training data, the outputs of the language model may not be correct. Subword vocabularies have emerged as a sweet-spot between these two extremes and are widely used in language models [Schuster and Nakajima, 2012, Sennrich et al., 2015, Kudo, 2018, Provilkov et al., 2020, He et al., 2020].

Given a long sequence of tokens and an initial fixed vocabulary, BPE consists of two core operations: (i) compute the most frequent pair of neighboring tokens and add it to the vocabulary, and (ii) merge all instances of the pair in the sequence. These two steps of adding tokens and making merges alternate until a fixed maximum vocabulary size is reached.

3.2 Discretizing the Action Space

In order to run BPE, it is necessary to have an initial vocabulary $\mathcal{V}$ as well as a string of discrete tokens. In a continuous action space, one simple way to form tokens is through clustering. Prior work has leveraged these ideas in similar contexts [Janner et al., 2021, Shafiullah et al., 2022, Jiang et al., 2022] and we follow suit. For simplicity, we perform k-means clustering with the Euclidean metric on the actions of demonstrations in $\mathcal{D}$ to form a vocabulary of k discrete tokens $\mathcal{V} = \{v_0, \dots, v_k\}$. Our default choice for k will be two times the number of degrees-of-freedom (DoF) of the original action space, or $2 \cdot d_{\text{act}}$. We will further study this choice in Appendix A.1. Such clustering is the same as the action space of Shafiullah et al. [2022] without the residual correction.

3.3 Scoring Merges

In NLP, we often have access to a large amount of text data from (mostly) correct human authors. However, for robotics applications we may not have the same quantity of near-optimal (or even suboptimal) demonstrations. As a result, it may be undesirable to merge tokens based on frequency alone. Thus, in addition to merging based on frequency, we implement a variant of our method that merges based on a proxy for the distance traveled in the observation space in order to encourage the creation of skills that explore diversely in state space and thus are efficient for tasks. We take inspiration from LSD [Park et al., 2022] and CSD [Park et al., 2023] for this choice. At the high sampling rate of continuous control observations, the observation space should be locally Euclidean, so euclidean distance makes sense as long as the length of skills is short enough. We label the two variants of our method as **SaS-freq** and **SaS-dist** respectively (SaS for Subwords as Skills).

Algorithm 1 Subword merging and pruning

Given dataset $\mathcal{D} = \{(o_{ij}, a_{ij})_i | i \in \mathbb{N} \cap [0, N),\ j \in \mathbb{N} \cap [0, n_i),\ o_{ij} \in \mathbb{R}^{d_{\text{obs}}},\ a_{ij} \in \mathbb{R}^{d_{\text{act}}}\}$
Given k, N_{max}, N_{min}, $\epsilon \ll 1$
Run k-means on actions with k clusters to get tokens $\mathcal{V} = \{v_i\}_{i=1}^k$
Tokenize $\mathcal{D}$ according to $\mathcal{V}$
Initialize $\mathcal{W} = \{w_i\}_{i=1}^k \leftarrow \mathcal{V}$, $\mathcal{Q} \leftarrow \varnothing$, $\bar{q} = 0$, $\Sigma_q = I$
// Merge vocabulary
while $|\mathcal{W}| < N_{\text{max}}$ **do**
  $\mathcal{W}' \leftarrow \{\text{All possible merges } w = \text{concat}(w_1, w_2) \text{ in } \mathcal{D} \mid w_1, w_2 \in \mathcal{W}\}$ // Get candidates
  for $w' \in \mathcal{W}'$ **do**
    Compute $q_{w'} = \mathbb{E}_{\text{instances of } w' \text{ in } \mathcal{D}} \left[\frac{1}{L} \sum_{r=1}^{L = \text{length of } w'} o_{ir} - o_{i1} \right]$ // Compute vectors
  end for
  $w' = \arg\max_{w' \in \mathcal{W}'} (q_{w'} - \bar{q})^\top \Sigma_q^{-1} (q_{w'} - \bar{q})$ // Find best possible merge
  $\mathcal{W} \leftarrow \mathcal{W} \cup \{w'\}$, $\mathcal{Q} \leftarrow \mathcal{Q} \cup \{q_{w'}\}$ // Add merge to vocabulary
  $\bar{q} \leftarrow \mathbb{E}_{q \in \mathcal{Q}}[q]$, $\Sigma_q \leftarrow \text{Cov}_{q \in \mathcal{Q}}(q) + \epsilon I$ // Update vocabulary mean and covariance
  Retokenize $\mathcal{D}$ according to $\mathcal{W}$
end while
// Prune vocabulary
while $|\mathcal{W}| > N_{\text{min}}$ **do**
  $w' = \arg\min_{w' \in \mathcal{W}} (q_{w'} - \bar{q})^\top \Sigma_q^{-1} (q_{w'} - \bar{q})$ // Find most redundant subword
  $\mathcal{W} \leftarrow \mathcal{W} \setminus \{w'\}$, $\mathcal{Q} \leftarrow \mathcal{Q} \setminus \{q_{w'}\}$ // Remove worst
  $\bar{q} \leftarrow \mathbb{E}_{q \in \mathcal{Q}}[q]$, $\Sigma_q \leftarrow \text{Cov}_{q \in \mathcal{Q}}(q) + \epsilon I$ // Update vocabulary mean and covariance
end while

return $\mathcal{W}$

More formally, suppose that two neighboring subwords w_1 and w_2 correspond to the trajectories $\tau_1 = \{(o_1, a_1), \ldots, (o_n, a_n)\}$ and $\tau_2 = \{(o_{n+1}, a_{n+1}), \ldots, (o_m, a_m)\}$. For an instance of the subword $w = \text{concat}(w_1, w_2)$ consisting of the entire trajectory $\tau = \text{concat}(\tau_1, \tau_2)$, we associate the vector $q_\tau = \frac{1}{m} \sum_{i=1}^m (o_i - o_1)$. This vector is analogous to the average "heading" of the subword, which ignores possible high-frequency, periodic motion like legs moving up and down. In order to obtain a vector that summarizes w, we compute the mean of such instances $q_w = \mathbb{E}_{(\tau_1, \tau_2) \in \mathcal{D}}[q_\tau]$, which takes into account possible observation noise at different instances.

Given an existing vocabulary of subwords $\mathcal{W} = \{w_0, \ldots, w_{n-1}\}$ and their corresponding vectors $\mathcal{Q} = \{q_0, \ldots, q_{n-1}\}$, we compute the mean $\bar{q} = \mathbb{E}_{q \in \mathcal{Q}}[q]$ and covariance matrix $\Sigma_q = \text{Cov}_{q \in \mathcal{Q}}(q) + \epsilon I$ for small ϵ. We associate a score to each possible new subword according to the Mahalanobis distance between the candidate subword and the set of existing subwords: $d_w = (q_w - \bar{q})^\top \Sigma_q^{-1} (q_w - \bar{q})$. We add the subword with maximum distance d_w to our vocabulary. We update Σ_q and $\bar{q}$ at every iteration. These steps yield a growing vocabulary of subwords that achieve high distance and diversity in observation space. Such a scoring function also accounts for the fact that different parts of the observation space may have different natural scales. We merge up to a maximum vocabulary size $|\mathcal{W}| = N_{\text{max}}$. The choice of N_{max} is studied in Appendix A.2.

3.4 Pruning the Subwords

If we stopped after merging to a maximum size, the final vocabulary would contain the intermediate subwords that make up the longest units. In the context of NLP, this redundancy may not be particularly detrimental. In reinforcement learning, however, redundancy in the action space of a new policy will result in similar actions competing for probability mass, making exploration and optimization more difficult. Thus we propose pruning the vocabulary.

For frequency-based merging, we begin with the longest subword, and remove subwords that are strictly contained, then move to the next longest and repeat the process. We do this until we reach the desired vocabulary size N_{min}.

For distance-based merging, we prune the set of subwords using the same metric as was used to merge. In particular, we find $w' = \arg\min_w d_w$, update $\mathcal{W} \leftarrow \mathcal{W} \setminus \{w'\}$, and recompute Σ_q and

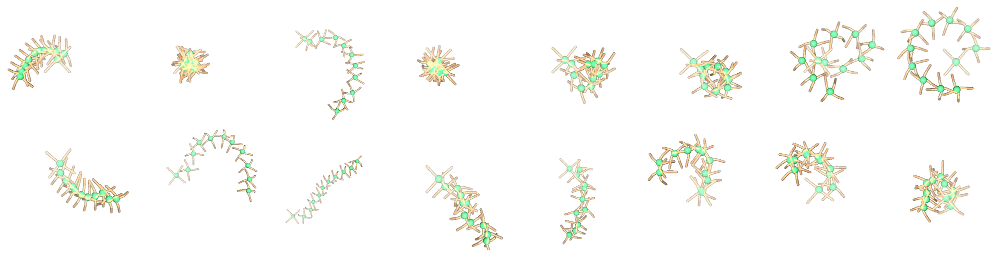

Figure 3: All skills generated for `antmaze-medium-diverse` where the transparency is higher for poses earlier in the trajectory. See Appendix B for more details.

$\bar{q}$. We continue pruning in this fashion until reaching a minimum vocabulary size $|\mathcal{W}| = N_{\text{min}}$. Finally, $\mathcal{W}$ becomes the action space for a new policy. Algorithm 1 provides the pseudocode for the distance-based method, and Figure 2 provides a graphical representation. We ablate the choice of N_{min} in Appendix A.3.

Implicit in our method is an assumption that portions of the demonstrations can be recomposed to solve a new task, i.e., that there exists a policy that solves the new task with this new action space. One can imagine a counter-example where the subwords we obtain lack some critical action sequence without which the task cannot be solved. Still, we will show that this is a reasonable assumption for several sparse-reward tasks.

4 Experiments

In the following sections, we explore the empirical performance of our proposed method: first extracting skills from data, then using those skills as an action space for learning a new policy through sparse-reward RL. We see that there are significant speed and performance benefits, with strong exploration behavior. We also discuss benefits and drawbacks of our unconditional skills when compared to conditional skills like those of SPiRL [Pertsch et al., 2021].

4.1 Reinforcement Learning with Unconditional Skills

Table 1: Main comparison (unnormalized scores). SSP corresponds to results from official code of Pertsch et al. [2021]. We report numbers at the end of training for consistency. SFP takes so long it is unmanageable on many domains. AntMaze is scored 0–1, Kitchen is scored 0–4 in increments of 1, CoinRun is scored 0–100 in increments of 10. *CoinRun is a discrete-action domain, so instead of SAC only SAC-discrete can be used. SSP results exist for Kitchen, ($0.8{\pm}0.2$ [Pertsch et al., 2021, Figure 4]), but we are unable to reproduce this number using official code.

Task	SAC	SAC-discrete	SSP	SFP	SaS-freq	SaS-dist
`antmaze-umaze-diverse`	0.0	0.0	0.0	—	0.0	$\mathbf{0.76}{\pm}\mathbf{0.43}$
`antmaze-medium-diverse`	0.0	0.0	0.0	0.0	0.0	$\mathbf{0.40}{\pm}\mathbf{0.55}$
`antmaze-large-diverse`	0.0	0.0	0.0	0.0	0.0	$\mathbf{0.34}{\pm}\mathbf{0.46}$
`kitchen-mixed`	0.0	0.0	0.0*	$0.12{\pm}0.07$	$0.16{\pm}0.17$	$\mathbf{0.72}{\pm}\mathbf{0.40}$
`CoinRun`	—*	0.0	$\mathbf{5.3}{\pm}\mathbf{3.4}$	0.0	$4.90{\pm}9.10$	$2.9{\pm}2.9$

Tasks: We consider AntMaze and Kitchen from D4RL [Fu et al., 2020], two challenging sparse-reward state-based tasks/datasets. AntMaze is a maze navigation task with a quadrupedal robot where the reward is 0 except for at the goal, and Kitchen is a manipulation task in a kitchen setting where reward is 0 except for on successful completion of a subtask. Demonstrations in AntMaze consist of random start and end states in the same maze, while demonstrations in Kitchen consist of different sequences of subtasks than the eventual task. We also consider CoinRun [Cobbe et al., 2019], a discrete-action platforming game. Unlike AntMaze and Kitchen, CoinRun is a visual domain and the demonstrations are collected in distinct levels than the final task. All of these domains require many coordinated actions in sequence to achieve any reward, with horizons between 280 and 1000 steps. See Appendix E for more information on the data.

Baselines: We consider SAC [Haarnoja et al., 2018b]; SAC-discrete [Christodoulou, 2019] on top of our discretized k-means actions; Skill-Space Policy (SSP), a VAE trained on sequences of 10 actions at a time [Pertsch et al., 2021]; and State-Free Priors (SFP) [Bagatella et al., 2022] a sequence model of actions that is used to inform action-selection during SAC inference, which takes the last action as context. For SAC, SAC-discrete, SSP, and SFP, we implement or run the official code with the default hyperparameters listed in the respective papers. Complete results are available in Table 1. All numbers are taken from the end of training. We report mean and standard deviation across five seeds. As defaults we use $k = 2 \cdot d_{\text{act}}$ and $N_{\text{min}} = 16$. We pick N_{max} per-domain such that skill lengths are comparable with SSP's length 10. For more experimental details see Appendix E. Including our method, all skills are not conditioned on observations.

We see in Table 1, that even in these challenging sparse-reward tasks, our method is the only one that is able to achieve nonzero reward across all tasks. All settings with zero reward fail to achieve any reward during training. The large standard deviations are due to the fact that some seeds fail to achieve any reward. Figure 3 visualizes 200-step rollouts of all of the discovered subwords for `antmaze-medium-diverse`. We provide mean and standard deviations for subword lengths in extracted vocabularies in Table 2. Failures of frequency-based merging in AntMazes are directly attributable to the discovery of long, constant sequences of actions, likely due to suboptimal demonstration trajectories that often jitter in place.

Table 2: Per-domain subword lengths. Numbers are intended to match the length-10 skills of SSP, but it is difficult to precisely control length due to the merging and pruning process.

Task	Subword length
`antmaze-umaze-diverse`	11.3±5.6
`antmaze-medium-diverse`	8.5±5.0
`antmaze-large-diverse`	12.5±5.3
`kitchen-mixed`	9.2±4.5
`CoinRun`	9.1±5.6

Due to the simplicity of our method, it also enjoys significant acceleration compared to the baselines. In Table 3, we measure the wall-clock time required to generate skills, as well as inference for a single rollout. We see that our method achieves extremely significant speedups compared to prior work, achieving both faster and more efficient learning, as well as faster inference during execution. Our skill discovery is fast as we simply need to run k-means and tokenization. SSP and SFP require training larger generative models. In the case of rollouts our method predicts an entire sequence of actions using a simple policy every 10 steps or so, while SSP and SFP require much larger models in order to predict the latent variable, and then generate the next action from that latent. The speedup of our method also translates to faster RL (around 10 hours for our method vs. 12 hours for SSP and 1 week for SFP).

Table 3: Timing on `antmaze-medium-diverse` in seconds. Methods measured on the same Nvidia RTX 3090 GPU with 8 Intel Core i7-9700 3 GHz CPUs @ 3.00 GHz. SSP takes around 36 hours for skill generation and SFP takes around 2 hours.

Method	Skill Generation	Online Rollout
SSP	130000±1800	0.9±0.05
SFP	8000±500	4.1±0.1
SaS-dist	**210**±10	**0.007**±0.0006

4.2 Exploration Behavior on AntMaze Medium

The stringent evaluation procedure for sparse-reward RL equally penalizes poor learning and exploration. In order to shed light on the many zeros in Table 1, we examine the exploration behavior on AntMaze Medium. We choose this domain because it is particularly straightforward to interpret what good and bad exploration looks like: coverage of the maze. In Figure 4 and Figure 5 we plot state visitation for the first 1 million of 10 million steps of RL. We show the approximate start position in grey in the bottom left and the approximate goal location in green in the top right. Higher color intensity (saturation) corresponds to a higher probability of that state. Color is scaled nonlinearly according to a power law between 0 and 1 for illustration purposes. Thin white areas between the density and the walls can be attributed to the fact that we plot the center body position, and the legs have a nontrivial size limiting the proximity to the wall.

In Figure 4, we show the exploration behavior across methods, averaged over 5 seeds. We see that the 0 values for the final reward in Table 1 for SAC, SSP and SFP are likely due not to poor optimization,

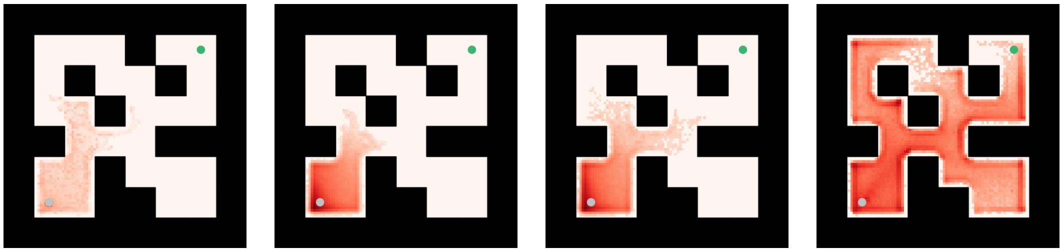

(a) SAC-discrete (b) SFP (c) SSP (d) SaS-dist

Figure 4: A visualization of state visitation for RL on `antmaze-medium-diverse` in the first 1 million timesteps for (a) SAC-discrete, (b) SFP, (c) SSP, and (d) our method. The grey circle in the bottom-left denotes the start position, while the green circle in the top-right indicates the goal. Notice that our method explores the maze much more extensively. SAC's visitation is tightly concentrated on the start state, which is why there is so little red in (a).

(a) Seed 0 (b) Seed 1 (c) Seed 2 (d) Seed 3 (e) Seed 4

Figure 5: State visitation achieved with our method for each of the 5 individual seeds. Notice the diversity of exploration behavior. This is true even for seeds 0, 2 and 3 that, as reflected in the standard deviations in Table 1, eventually finish with a final reward of 0.

but rather poor exploration early in training, unlike our method. One reason for this could be due to the fact that our subwords are a discrete set, so policy exploration does not include small differences in a continuous space. In addition, SAC has fundamental issues in sparse-reward environments as the signal to the Q function is driven entirely by the entropy bonus, which will lead to uniform weighting on every action and as a result Brownian motion in the action space. Such behavior is likely why the default setting for SAC [Haarnoja et al., 2018b] aggressively drives the policy to determinism, but in the sparse reward setting this also results in a uniform policy. Without long sequences of coordinated actions such exploration is insufficient.

In Figure 5, we show the individual seed visitation of our method in the first 1 million steps. This is to demonstrate that, even though individual seeds may have some bias, they all are able to explore much more widely than the collective exploration of baseline methods. Indeed, this suggests that the large standard deviations of our method are a result of an optimization failure, as suggested by Zhou et al. [2022], and not poor exploration due to bad skill-encoding.

4.3 Comparison to Observation-Conditioned Skills

Our method for extracting skills is an unconditional, open-loop method with the objective that the skills should generalize. Still, this comes with the drawback that a policy needs to learn the context to deploy skills from scratch. Alternatively, observation-conditioned skills bias policy exploration to match that of the demonstrations. This allows for more stable exploration, but worse generalization [Bagatella et al., 2022].

Baselines: Here we compare to observation-conditioned extension of SSP, SPiRL and SPiRL-cl (the closed-loop version) [Pertsch et al., 2021, 2022] which bias a policy toward skills used in the exact context of demonstrations in the dataset. We also include OPAL [Ajay et al., 2020], a conditional flow model similar to SPiRL. We take numbers from the paper as OPAL is closed-source.

In Table 4, we see that SPiRL and SPiRL-cl show very strong performance on Kitchen, where the overlap between the dataset and the downstream task is exact, but SPiRL fails on AntMaze-large,

Table 4: Comparison to methods with observation-conditioned skills. In general we see conditioning helps when the data closely overlaps with the downstream task (Kitchen), but not in CoinRun where such an overlap cannot be assumed. With AntMaze the results are mixed likely due to the suboptimal quality of the demonstrations. We highlight that, even without conditioning, our method is competitive in AntMaze-large and comparable to SPiRL in AntMaze-medium. OPAL is a closed-source method similar to SPiRL, and results are from Ajay et al. [2020].

Task	SPiRL	SPiRL-cl	OPAL	SaS-freq	SaS-dist
`antmaze-medium-diverse`	0.40 ± 0.49	1.00 ± 0.00	0.82 ± 0.04	0.0	0.40 ± 0.55
`antmaze-large-diverse`	0.0	0.20 ± 0.40	0.0	0.0	0.34 ± 0.46
`kitchen-mixed`	1.87 ± 0.16	3.00 ± 0.00	—	0.16 ± 0.17	0.72 ± 0.40
`CoinRun`	5.32 ± 5.41	0.0	—	4.90 ± 9.10	2.90 ± 2.90

while SPiRL-cl fails on CoinRun, likely due to differences between the dataset for CoinRun (easy levels) and the downstream task (hard levels). In addition, notice that BPE with simple frequency merging (SaS-freq) is poor in AntMaze as discussed previously but comparable in CoinRun. We are able to replicate results for SPiRL-cl (2–3 in the original paper [Pertsch et al., 2022]), but for SPiRL our result is significantly worse (2–3 in the original paper [Pertsch et al., 2021]). Given we use the official code which already implements Kitchen, the difficulty of sparse-reward is likely to blame.

In addition, we examine generalization behavior across observation-conditioned methods. Table 5 highlights the drawback that conditioning has in generalization. In particular the strongest advantage for conditional skills is in a setting where the data closely matches the final task, but it may be detrimental when we do not have access to sufficiently general demonstrations, like the ∼10,000 trajectories in randomized environments that SPiRL uses for visual PointMaze [Pertsch et al., 2021].

Table 5: Results on transferring skills extracted from `antmaze-medium-diverse` to downstream RL on `antmaze-umaze-diverse`. We see that methods with conditioning (SPiRL and SPiRL-cl) underperform our simple unconditional method. Similar conclusions were drawn by the authors of SFP [Bagatella et al., 2022, Figures 7, 16], where stronger conditioning fails to generalize.

Task	SSP	SPiRL	SPiRL-cl	SaS-dist
`antmaze-medium-diverse` → `antmaze-umaze-diverse`	0.0	0.60 ± 0.49	0.20 ± 0.40	$\mathbf{0.97 \pm 0.12}$

5 Conclusion

Limitations: As proposed, there are a few key limitations to our method. Discretization removes resolution from the action space, which may be detrimental in settings like fast locomotion (Appendix H), but this may be fixed by more clusters or a residual correction [Shafiullah et al., 2022]. In addition, like prior work execution of our subwords is open loop, so exploration can be inefficient [Amin et al., 2020] and unsafe [Park et al., 2021]. Finally, in order to operate on the CoinRun domain, we downsample inputs from 64×64 resolution to 32×32 to make matrix inversion during merging less expensive (2 hours vs. 2 minutes). In high-dimensional visual input domains, our merging may be too computationally expensive to perform. However, this can be resolved by using neural network features instead of images. We also speculate that higher-quality demonstrations could allow us to generate skills simply by merging based on frequency (Table 1, CoinRun), and these demonstrations may be easy to obtain if they don't need to be collected in the deployment domain (Table 5).

Architectures from NLP have made their way into offline RL [Chen et al., 2021, Janner et al., 2021, Shafiullah et al., 2022], but as we have demonstrated, there is a trove of further techniques to explore. Given prior evidence that the full range of the action space is not required, we discretize and form skills through a simple tokenization method. Such a method is much faster both in skill generation and in policy inference, and leads to strong performance in a relatively small sample budget on several challenging sparse-reward tasks. Moreover, the discrete nature of our skills lends itself to interpretation: one can simply look at the execution to figure out what has been extracted (Appendix B). Given its many advantages, we believe that such a tokenization method is the first step on a new road to efficient reinforcement learning.

References

J. Achiam and S. Sastry. Surprise-based intrinsic motivation for deep reinforcement learning. *arXiv preprint arXiv:1703.01732*, 2017.

A. Ajay, A. Kumar, P. Agrawal, S. Levine, and O. Nachum. OPAL: Offline primitive discovery for accelerating offline reinforcement learning. *arXiv preprint arXiv:2010.13611*, 2020.

S. Amin, M. Gomrokchi, H. Aboutalebi, H. Satija, and D. Precup. Locally persistent exploration in continuous control tasks with sparse rewards. *arXiv preprint arXiv:2012.13658*, 2020.

M. Andrychowicz, F. Wolski, A. Ray, J. Schneider, R. Fong, P. Welinder, B. McGrew, J. Tobin, P. Abbeel, and W. Zaremba. Hindsight experience replay. *arXiv preprint arXiv:1707.01495*, 2017.

P.-L. Bacon, J. Harb, and D. Precup. The option-critic architecture. In *Proceedings of the National Conference on Artificial Intelligence (AAAI)*, pages 1726–1734, 2017.

M. Bagatella, S. Christen, and O. Hilliges. SFP: State-free priors for exploration in off-policy reinforcement learning. *Transactions on Machine Learning Research*, 2022.

A. G. Barto and S. Mahadevan. Recent advances in hierarchical reinforcement learning. *Discrete event dynamic systems*, 13:41–77, 2003.

M. Bellemare, S. Srinivasan, G. Ostrovski, T. Schaul, D. Saxton, and R. Munos. Unifying count-based exploration and intrinsic motivation. In *Advances in Neural Information Processing Systems (NeurIPS)*, 2016.

L. Biewald. Experiment tracking with weights and biases, 2020. URL https://www.wandb.com/. Software available from wandb.com.

C. Boutilier, R. I. Brafman, and C. Geib. Prioritized goal decomposition of Markov decision processes: Toward a synthesis of classical and decision theoretic planning. In *Proceedings of the International Joint Conference on Artificial Intelligence (IJCAI)*, pages 1156–1162, 1997.

Y. Burda, H. Edwards, D. Pathak, A. Storkey, T. Darrell, and A. A. Efros. Large-scale study of curiosity-driven learning. *arXiv preprint arXiv:1808.04355*, 2018a.

Y. Burda, H. Edwards, A. Storkey, and O. Klimov. Exploration by random network distillation. *arXiv preprint arXiv:1810.12894*, 2018b.

L. Chen, K. Lu, A. Rajeswaran, K. Lee, A. Grover, M. Laskin, P. Abbeel, A. Srinivas, and I. Mordatch. Decision transformer: Reinforcement learning via sequence modeling. In *Advances in Neural Information Processing Systems (NeurIPS)*, pages 15084–15097, Dec. 2021.

N. Chentanez, A. Barto, and S. Singh. Intrinsically motivated reinforcement learning. In *Advances in Neural Information Processing Systems (NeurIPS)*, 2004.

P. Christodoulou. Soft actor-critic for discrete action settings. *arXiv preprint arXiv:1910.07207*, 2019.

K. Cobbe, O. Klimov, C. Hesse, T. Kim, and J. Schulman. Quantifying generalization in reinforcement learning. In *International Conference on Machine Learning*, pages 1282–1289, 2019.

R. Dadashi, L. Hussenot, D. Vincent, S. Girgin, A. Raichuk, M. Geist, and O. Pietquin. Continuous control with action quantization from demonstrations. In *International Conference on Machine Learning*, pages 4537–4557, 2022.

C. Daniel, G. Neumann, and J. Peters. Hierarchical relative entropy policy search. In *Proceedings of the International Conference on Artificial Intelligence and Statistics (AISTATS)*, pages 273–281, 2012.

P. Dayan and G. E. Hinton. Feudal reinforcement learning. In *Advances in Neural Information Processing Systems (NeurIPS)*, 1992.

T. G. Dietterich. Hierarchical reinforcement learning with the MAXQ value function decomposition. *Journal of Artificial Intelligence Research*, 13:227–303, November 2000.

S. Emmons, B. Eysenbach, I. Kostrikov, and S. Levine. RvS: What is essential for offline RL via supervised learning? *arXiv preprint arXiv:2112.10751*, 2021.

B. Eysenbach, A. Gupta, J. Ibarz, and S. Levine. Diversity is all you need: Learning skills without a reward function. *arXiv preprint arXiv:1802.06070*, 2018.

W. A. Falcon. PyTorch Lightning. https://lightning.ai.

J. Fu, A. Kumar, O. Nachum, G. Tucker, and S. Levine. D4RL: Datasets for deep data-driven reinforcement learning. *arXiv preprint arXiv:2004.07219*, 2020.

P. Gage. A new algorithm for data compression. *C Users Journal*, 12(2):23–38, 1994.

K. Gregor, D. J. Rezende, and D. Wierstra. Variational intrinsic control. *arXiv preprint arXiv:1611.07507*, 2016.

S. Gu, E. Holly, T. Lillicrap, and S. Levine. Deep reinforcement learning for robotic manipulation with asynchronous off-policy updates. In *Proceedings of the IEEE International Conference on Robotics and Automation (ICRA)*, pages 3389–3396, 2017.

T. Haarnoja, S. Ha, A. Zhou, J. Tan, G. Tucker, and S. Levine. Learning to walk via deep reinforcement learning. *arXiv preprint arXiv:1812.11103*, 2018a.

T. Haarnoja, A. Zhou, K. Hartikainen, G. Tucker, S. Ha, J. Tan, V. Kumar, H. Zhu, A. Gupta, P. Abbeel, and S. Levine. Soft actor-critic algorithms and applications. *arXiv preprint arXiv:1812.05905*, 2018b.

N. Haber, D. Mrowca, S. Wang, L. F. Fei-Fei, and D. L. Yamins. Learning to play with intrinsically-motivated, self-aware agents. In *Advances in Neural Information Processing Systems (NeurIPS)*, Montréal, Canada, Dec. 2018.

E. Hazan, S. Kakade, K. Singh, and A. Van Soest. Provably efficient maximum entropy exploration. In *Proceedings of the International Conference on Machine Learning (ICML)*, pages 2681–2691, 2019.

X. He, G. Haffari, and M. Norouzi. Dynamic programming encoding for subword segmentation in neural machine translation. In *Proceedings of the Association for Computational Linguistics (ACL)*, pages 3042–3051, 2020.

P. Henderson, R. Islam, P. Bachman, J. Pineau, D. Precup, and D. Meger. Deep reinforcement learning that matters. In *Proceedings of the National Conference on Artificial Intelligence (AAAI)*, 2018.

M. Janner, Q. Li, and S. Levine. Offline reinforcement learning as one big sequence modeling problem. In *Advances in Neural Information Processing Systems (NeurIPS)*, pages 1273–1286, 2021.

M. Janner, Y. Du, J. B. Tenenbaum, and S. Levine. Planning with diffusion for flexible behavior synthesis. *arXiv preprint arXiv:2205.09991*, 2022.

Z. Jiang, T. Zhang, M. Janner, Y. Li, T. Rocktäschel, E. Grefenstette, and Y. Tian. Efficient planning in a compact latent action space. *arXiv preprint arXiv:2208.10291*, 2022.

L. P. Kaelbling. Hierarchical learning in stochastic domains: Preliminary results. In *Proceedings of the International Conference on Machine Learning (ICML)*, pages 167–173, 1993.

D. P. Kingma and J. Ba. Adam: A method for stochastic optimization. *arXiv preprint arXiv:1412.6980*, 2014.

G. Konidaris and A. Barto. Skill discovery in continuous reinforcement learning domains using skill chaining. In *Advances in Neural Information Processing Systems (NeurIPS)*, December 2009.

T. Kudo. Subword regularization: Improving neural network translation models with multiple subword candidates. In *Proceedings of the Association for Computational Linguistics (ACL)*, pages 66–75, 2018. doi: 10.18653/v1/P18-1007.

T. D. Kulkarni, K. R. Narasimhan, A. Saeedi, and J. B. Tenenbaum. Hierarchical deep reinforcement learning: Ingegrating temporal abstaction and intrinsic motivation. In *Advances in Neural Information Processing Systems (NeurIPS)*, Barcelona, Spain, December 2016.

A. Kumar, A. Zhou, G. Tucker, and S. Levine. Conservative Q-learning for offline reinforcement learning. In *Advances in Neural Information Processing Systems (NeurIPS)*, pages 1179–1191, 2020.

R. T. Lange and A. Faisal. Semantic rl with action grammars: Data-efficient learning of hierarchical task abstractions. *arXiv preprint arXiv:1907.12477*, 2019.

L. Lee, B. Eysenbach, E. Parisotto, E. Xing, S. Levine, and R. Salakhutdinov. Efficient exploration via state marginal matching. *arXiv preprint arXiv:1906.05274*, 2019.

A. Levy, G. Konidaris, R. Platt, and K. Saenko. Learning multi-level hierarchies with hindsight. *arXiv preprint arXiv:1712.00948*, 2017.

H. Liu and P. Abbeel. Behavior from the void: Unsupervised active pre-training. In *Advances in Neural Information Processing Systems (NeurIPS)*, pages 18459–18473, 2021.

M. Lopes, T. Lang, M. Toussaint, and P.-Y. Oudeyer. Exploration in model-based reinforcement learning by empirically estimating learning progress. In *Advances in Neural Information Processing Systems (NeurIPS)*, 2012.

C. Lynch, M. Khansari, T. Xiao, V. Kumar, J. Tompson, S. Levine, and P. Sermanet. Learning latent plans from play. In *Proceedings of the Conference on Robot Learning (CoRL)*, pages 1113–1132, 2020.

V. Mnih, K. Kavukcuoglu, D. Silver, A. Graves, I. Antonoglou, D. Wierstra, and M. A. Riedmiller. Playing atari with deep reinforcement learning. *arXiv:1312.5602*, 2013.

S. Mohamed and D. Jimenez Rezende. Variational information maximisation for intrinsically motivated reinforcement learning. In *Advances in Neural Information Processing Systems (NeurIPS)*, 2015.

O. Nachum, S. S. Gu, H. Lee, and S. Levine. Data-efficient hierarchical reinforcement learning. In *Advances in Neural Information Processing Systems (NeurIPS)*, Montréal, Canada, 2018.

S. Park, J. Kim, and G. Kim. Time discretization-invariant safe action repetition for policy gradient methods. In *Advances in Neural Information Processing Systems (NeurIPS)*, pages 267–279, 2021.

S. Park, J. Choi, J. Kim, H. Lee, and G. Kim. Lipschitz-constrained unsupervised skill discovery. In *International Conference on Learning Representations*, 2022.

S. Park, K. Lee, Y. Lee, and P. Abbeel. Controllability-aware unsupervised skill discovery. *arXiv preprint arXiv:2302.05103*, 2023.

R. Parr and S. Russell. Reinforcement learning with hierarchies of machines. In *Advances in Neural Information Processing Systems (NeurIPS)*, pages 1043–1049, 1997.

R. E. Parr. *Hierarchical control and learning for Markov decision processes*. PhD thesis, University of California, Berkeley, Berkeley, CA, 1998.

A. Paszke, S. Gross, F. Massa, A. Lerer, J. Bradbury, G. Chanan, T. Killeen, Z. Lin, N. Gimelshein, L. Antiga, et al. PyTorch: An imperative style, high-performance deep learning library. In *Advances in Neural Information Processing Systems (NeurIPS)*, 2019.

D. Pathak, P. Agrawal, A. A. Efros, and T. Darrell. Curiosity-driven exploration by self-supervised prediction. In *Proceedings of the International Conference on Machine Learning (ICML)*, pages 2778–2787, 2017.

F. Pedregosa, G. Varoquaux, A. Gramfort, V. Michel, B. Thirion, O. Grisel, M. Blondel, P. Prettenhofer, R. Weiss, V. Dubourg, J. Vanderplas, A. Passos, D. Cournapeau, M. Brucher, M. Perrot, and E. Duchesnay. Scikit-learn: Machine learning in Python. *Journal of Machine Learning Research*, 12:2825–2830, 2011.

K. Pertsch, Y. Lee, and J. Lim. Accelerating reinforcement learning with learned skill priors. In *Proceedings of the Conference on Robot Learning (CoRL)*, pages 188–204, 2021.

K. Pertsch, Y. Lee, Y. Wu, and J. J. Lim. Guided reinforcement learning with learned skills. In *Conference on Robot Learning*, pages 729–739, 2022.

S. Pitis, H. Chan, S. Zhao, B. Stadie, and J. Ba. Maximum entropy gain exploration for long horizon multi-goal reinforcement learning. In *Proceedings of the International Conference on Machine Learning (ICML)*, pages 7750–7761, 2020.

P. Poupart, N. Vlassis, J. Hoey, and K. Regan. An analytic solution to discrete Bayesian reinforcement learning. In *Proceedings of the International Conference on Machine Learning (ICML)*, pages 697–704, Pittsburgh, PA, 2006.

I. Provilkov, D. Emelianenko, and E. Voita. BPE-dropout: Simple and effective subword regularization. In *Proceedings of the Association for Computational Linguistics (ACL)*, pages 1882–1892, 2020.

A. Raffin, A. Hill, A. Gleave, A. Kanervisto, M. Ernestus, and N. Dormann. Stable-Baselines3: Reliable reinforcement learning implementations. *Journal of Machine Learning Research*, 22(268), 2021.

J. Schmidhuber. A possibility for implementing curiosity and boredom in model-building neural controllers. In *Proceedings of the International Conference on Simulation of Adaptive Behavior: From Animals to Animats (SAB)*, pages 222–227, 1991.

M. Schuster and K. Nakajima. Japanese and korean voice search. In *Proceedings of the IEEE International Conference on Acoustics, Speech and Signal Processing (ICASSP)*, pages 5149–5152, 2012.

R. Sennrich, B. Haddow, and A. Birch. Neural machine translation of rare words with subword units. *arXiv preprint arXiv:1508.07909*, 2015.

N. M. Shafiullah, Z. Cui, A. A. Altanzaya, and L. Pinto. Behavior transformers: Cloning k modes with one stone. In *Advances in Neural Information Processing Systems (NeurIPS)*, pages 22955–22968, New Orleans, LA, 2022.

A. Sharma, S. Gu, S. Levine, V. Kumar, and K. Hausman. Dynamics-aware unsupervised discovery of skills. *arXiv preprint arXiv:1907.01657*, 2019.

S. Sharma, A. Srinivas, and B. Ravindran. Learning to repeat: Fine grained action repetition for deep reinforcement learning. In *International Conference on Learning Representations*, 2017.

D. Silver, J. Schrittwieser, K. Simonyan, I. Antonoglou, A. Huang, A. Guez, T. Hubert, L. Baker, M. Lai, A. Bolton, Y. Chen, T. Lillicrap, F. Hui, L. Sifre, G. van den Driessche, T. Graepel, and D. Hassabis. Mastering the game of Go without human knowledge. *Nature*, 550(7676):354–359, 2017.

A. Singh, H. Liu, G. Zhou, A. Yu, N. Rhinehart, and S. Levine. Parrot: Data-driven behavioral priors for reinforcement learning. *arXiv preprint arXiv:2011.10024*, 2020.

B. C. Stadie, S. Levine, and P. Abbeel. Incentivizing exploration in reinforcement learning with deep predictive models. *arXiv preprint arXiv:1507.00814*, 2015.

R. S. Sutton. TD models: Modeling the world at a mixture of time scales. In *Proceedings of the International Conference on Machine Learning (ICML)*, pages 531–539. 1995.

R. S. Sutton, D. Precup, and S. Singh. Between MDPs and semi-MDPs: A framework for temporal abstraction in reinforcement learning. *Artificial Intelligence*, 112(1–2):181–211, August 1999.

A. S. Vezhnevets, S. Osindero, T. Schaul, N. Heess, M. Jaderberg, D. Silver, and K. Kavukcuoglu. FeUdal networks for hierarchical reinforcement learning. In *Proceedings of the International Conference on Machine Learning (ICML)*, pages 3540–3549, Sydney, Australia, Aug. 2017.

Z. Wang, J. J. Hunt, and M. Zhou. Diffusion policies as an expressive policy class for offline reinforcement learning. *arXiv preprint arXiv:2208.06193*, 2022.

D. Warde-Farley, T. Van de Wiele, T. Kulkarni, C. Ionescu, S. Hansen, and V. Mnih. Unsupervised control through non-parametric discriminative rewards. *arXiv preprint arXiv:1811.11359*, 2018.

D. Yarats, R. Fergus, A. Lazaric, and L. Pinto. Reinforcement learning with prototypical representations. In *Proceedings of the International Conference on Machine Learning (ICML)*, pages 11920–11931, July 2021.

H. Zhou, Z. Lin, J. Li, D. Ye, Q. Fu, and W. Yang. Revisiting discrete soft actor-critic. *arXiv preprint arXiv:2209.10081*, 2022.

Acknowledgments

We thank Takuma Yoneda and Jiading Fang as well as other members of the RIPL lab at TTIC for helpful discussions throughout the process. This material is based upon work supported by the National Science Foundation Graduate Research Fellowship Program under Grant No. 1754881. Any opinions, findings, and conclusions or recommendations expressed in this material are those of the authors and do not necessarily reflect the views of the National Science Foundation.

Division of Labor

DY came up with and implemented the method, adapted baseline code, ran most of the experiments and generated Kitchen visualizations. JJ adapted the SFP baseline to the settings considered and generated AntMaze subword visualizations. FD ran the initial CoinRun experiments to test feasibility, collected CoinRun trajectory data for use by all methods and made Figure 2. MW advised the project at every stage. DY and MW were responsible for most of the writing.

A Ablations

Certainly the level of discretization, and the size of the vocabulary will have an effect on performance. In the following sections we perform ablations over the primary hyperparameters on AntMaze-Medium and Kitchen.

A.1 Number of Discrete Primitives

All of our results in Table 1 use the simple rule-of-thumb that $k = 2 \times$ degrees-of-freedom. Such a choice may not be optimal depending on the setting. In Table 6 we see that this choice seems to be a simple sweet spot across the two domains, though the method can achieve reward with significantly different values of k.

Table 6: Results for different numbers of clusters in terms of the number of degrees-of-freedom (DoF). AntMaze DoF = 8, Kitchen DoF = 9. The default setting is in bold.

k	4	$1 \times$ DoF	**$2 \times$ DoF**	$4 \times$ DoF	$8 \times$ DoF
antmaze-medium-diverse	0.0	0.0	$0.40_{\pm 0.55}$	$0.20_{\pm 0.45}$	0.0
kitchen-mixed	$0.16_{\pm 0.35}$	$0.08_{\pm 0.18}$	$0.72_{\pm 0.40}$	0.0	$0.20_{\pm 0.45}$

A.2 Maximum Vocabulary Size

A crucial property of the vocabulary is the length of the subwords within. Long subwords lead to more temporal abstraction and easier credit-assignment for the policy, but long subwords can also get stuck for many transitions, leading to poor exploration. In Table 7, we vary the value of N_{max}, which is a proxy for the length of the subwords in the vocabulary. Our default setting for each environment targets an average length of around 10 to match the baselines, but we see that different domains may have different optimal choices for length, which makes sense given the episode length for Kitchen is around a quarter of that of AntMaze.

Table 7: Results for maximum vocabulary size (proxy for length).

N_{max}	32	64	128	256	512
antmaze-medium-diverse	0.0	$0.25_{\pm 0.5}$	$0.40_{\pm 0.55}$	$0.61_{\pm 0.48}$	$0.07_{\pm 0.08}$
kitchen-mixed	0.0	$0.50_{\pm 0.57}$	$0.72_{\pm 0.40}$	$0.04_{\pm 0.10}$	0.0

A.3 Minimum Vocabulary Size

Ultimately, the dimensionality of the action space will make exploration easier or harder. A large vocabulary results in too many paths for the policy to explore well, but a vocabulary that is too small

Table 8: Results for minimum vocabulary size N_{min}. In bold is the default setting.

N_{min}	4	6	8	12	**16**
antmaze-medium-diverse	0.0	0.24 ± 0.49	0.71 ± 0.41	0.41 ± 0.49	0.40 ± 0.55
kitchen-mixed	0.0	0.0	0.0	0.01 ± 0.01	0.72 ± 0.40

may not include all the subwords necessary to represent a good policy for the task. We see in Table 8 that even if AntMaze can be accomplished with fewer subwords (a smart handcrafted action space might consist of one action for turning and one for moving forward), Kitchen performance suffers significantly at low values.

B Qualitative Description of Skills

One nice property of our method is that, given that we create a finite and discrete vocabulary, we can inspect the discovered skills. Below, we discuss the AntMaze and Kitchen domains as an example. In order to visualize skills, we take the subwords and execute them for 200 steps in the environment, and visualize the resulting trajectory. It may be the case that the actual duration of a skill could be much shorter, but this is done to make the motions very clear.

In Figure 3 (main paper), we see all the skills extracted for a run of AntMaze. In particular, turning in both directions, with differing turn radii, as well as linear motions in different directions are discovered. It is straightforward to imagine why one would need both in designing an action space, and it seems that there are few explicit repetitions (though many variations on a theme) in the discovered skills. Also, as desired, the skills accomplish some coherent motion, instead of just repeating the same action and staying in place as a result, or falling over due to an unstable execution, or jittering randomly.

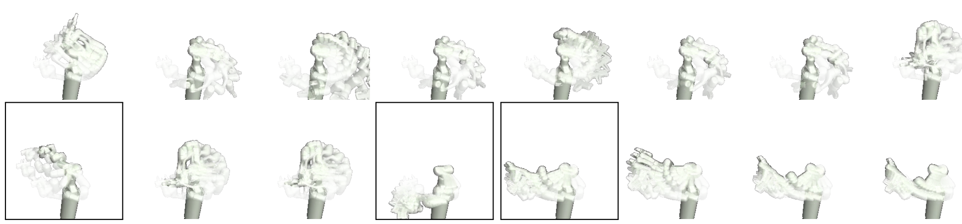

Figure 6: All skills generated for `kitchen-mixed-v0` where the transparency is higher for poses earlier in the trajectory. We see a range of different behaviors across the skills. Framed skills are highlighted in more detail in the text.

In Figure 6, we visualize the different skills discovered in the Kitchen domain. These are difficult to present in a static form, as it is not simple to visualize interaction with the environment, but they consist of a variety of reaching and rotational motions that are useful for interacting with different objects. In the bordered images, we highlight three particular skills. In the bottom left is a reaching skill that might be used for reaching the light switch/oven knobs. Next from the left is a turning skill that could be useful for adjusting some knob if the arm is in a particular position. Lastly there is a pulling skill, that might be useful for opening the microwave door. In general, these skills may not make sense unless the arm is already in a particular starting position, which makes visualizing them nontrivial.

C Discrete Actions from Data

Prior work combines discretization with many additional architectural and optimization components. To test the behavior of discrete actions in isolation, we perform behavior cloning with a simple fully-connected neural network on demonstration data from the D4RL [Fu et al., 2020] dataset. To be clear, our objective is not to show that simple k-means on demonstrations outperforms contemporary methods. Instead, we investigate whether behavioral cloning with these actions achieves modest

Table 9: D4RL offline learning results. BC numbers are from Emmons et al. [2021], Diffusion-QL numbers are from Wang et al. [2022], CQL numbers are from Kumar et al. [2020]. k-means BC numbers are from the checkpoint with the best average score during training.

Task	BC	k-means BC	CQL	Diffuser	Diffusion-QL	k-means BC + goals
hopper-medium	52.9	8.3±1.9	58.0	74.3±1.4	90.5±4.6	—
hopper-medium-replay	18.1	8.3±1.6	—	93.6±0.4	101.3±0.6	—
hopper-medium-expert	52.5	10.2±1.7	111.0	103.3±1.3	111.1±1.3	—
walker2d-medium	75.3	9.8±2.7	79.2	79.6±0.55	87.0±0.9	—
walker2d-medium-replay	26.0	7.9±0.7	0	70.6±1.6	95.5±1.5	—
walker2d-medium-expert	107.5	9.7±0.6	98.7	106.9±0.2	110.1±0.3	—
halfcheetah-medium	42.6	27.2±3.5	—	42.8±0.3	51.1±0.5	—
halfcheetah-medium-replay	36.6	8.6±2.8	—	37.7±0.5	47.8±0.3	—
halfcheetah-medium-expert	55.2	15.1±4.4	62.4	88.9±0.3	96.8±0.3	—
antmaze-umaze	54.6	84.0±8.3	74.0	—	93.4±3.4	82.6±6.6
antmaze-umaze-diverse	45.6	93.8±4.7	84.0	—	66.2±8.6	89.0±7.2
antmaze-medium-play	0.0	0.0	61.2	—	76.6±10.8	15.2±9.8
antmaze-medium-diverse	0.0	0.0	53.7	—	78.6±10.3	14.4±7.5
antmaze-large-play	0.0	0.0	15.8	—	46.4±8.3	2.6±2.8
antmaze-large-diverse	0.0	0.0	14.9	—	56.6±7.6	10.8±5.6
kitchen-complete	65.0	54.0±3.5	43.8	—	84.0±7.4	—
kitchen-partial	38.0	14.8±0.2	49.8	—	60.5±6.9	—
kitchen-mixed	51.5	18.0±4.6	—	—	62.6±5.1	—

performance in which case there is the potential for further tokenization to be effective in sparse-reward domains.

We compare to CQL [Kumar et al., 2020], an offline Q-learning algorithm that encourages staying close to the demonstration distribution; Diffuser [Janner et al., 2022], a diffusion model conditioned on an initial and final state; and Diffusion-QL [Wang et al., 2022], an offline Q-learning algorithm that uses a diffusion model on top of actions to stay close to the demonstration distribution. For more details on the experimental setting, see Appendix D.

In Table 9, we see that the dense-reward locomotion domains suffer from discretization, which makes sense as locomotion policies may require fine-grained control to move at high speed and achieve high reward. On AntMaze, however, we see that simple k-means discretization significantly boosts performance. This can be due to the fact that, at a given position, there are many possible motions that can move the body, but they are completely distinct in action space, which a unimodal policy may fail to capture. In the Kitchen domain, a policy that reasons over discrete actions achieves modest performance. The data in this domain was collected from expert human demonstrations, and there is very low variability in the executions, so it may be the case that multimodality is simply not necessary.

D Offline RL Experimental Details

D.1 Data

To measure the performance of behavior cloning with discrete actions, we take advantage of datasets from D4RL [Fu et al., 2020]. In particular, we select three subclasses of tasks. First are the MuJoCo dense-reward locomotion tasks, which consist of demonstrations collected from an RL agent, where `medium` refers to a policy partway through optimization, `medium-replay` refers to all samples in the replay buffer til the policy obtains `medium` performance, and `medium-expert` refers to a mix of data from an expert policy and a policy midway through training. Second are the AntMaze tasks, which are a collection of sparse-reward maze navigation tasks on top of the MuJoCo Ant quadrupedal robot. Demonstrations are either `play`, which is a scripted policy navigating between a couple fixed start and endpoints, which do not overlap with the final task, and `diverse`, which is the same scripted policy navigating between random start and endpoints. Third, are the Kitchen tasks, which are a collection of VR-collected demonstrations of subtasks in a Kitchen, where the final goal is to perform 4 in sequence. The settings include `complete` that consists of demonstrations of all subtasks in order, `partial` that consists of some sequences in the correct order, and others not, and `mixed` that consists of subtask demonstrations, some of which are unused for the final task.

(a) antmaze-medium (b) antmaze-large (c) kitchen (d) CoinRun

Figure 7: Offline environments, figures courtesy of Fu et al. [2020] and Cobbe et al. [2019]. For mazes, the starting locations are in the bottom left, and goals are in the top right.

To perform the goal-conditioned experiments for the AntMaze task, for each trajectory we extract the last state that is considered "terminal" (e.g., falling over or reaching the goal) and create a (state, action, goal) triplet for each transition in the trajectory.

D.2 Model

For the model, we choose a 4-layer MLP with 256 hidden units in each layer. We use the default initialization in Stable Baselines 3 [Raffin et al., 2021].

D.3 Optimization

We train our model with Adam [Kingma and Ba, 2014] with a learning rate of $3e-4$ and the default PyTorch [Paszke et al., 2019] betas. All numbers are reported for 5 random seeds with 300 epochs of training.

D.4 Choice of Number of Clusters

For the locomotion and AntMaze environments, we choose $k = 2\times$ the number of DoF. For Kitchen, we choose $k = 8\times$ DoF. This discrepancy is due to the fact that Kitchen performs poorly with the simple baseline choice. In particular we believe that this is due to the fact that Kitchen demonstrations are particularly good, and not particularly multimodal, so they benefit from the higher resolution that a larger k affords. This is similar to the hyperparameter settings of Shafiullah et al. [2022] in the same environment.

D.5 Implementation

Code was implemented in Python using PyTorch [Paszke et al., 2019] and PyTorch Lightning [Falcon] for deep learning, and Weights & Biases [Biewald, 2020] for logging.

D.6 Computational Requirements

All experiments were performed on an internal cluster with access to around 100 Nvidia 2080 Ti (or more capable) GPUs. Each single run fits in around 2 GB of GPU memory on a single machine. For supervised learning, training takes less than 2 hours on a single machine.

E Online RL Experimental Details

E.1 Data

As a set of diverse and challenging sparse-reward tasks, we select AntMaze and Kitchen from D4RL [Fu et al., 2020] and CoinRun [Cobbe et al., 2019].

AntMaze (Figs. 7(a) and 7(b)) is a task where a MuJoCo Ant robot is tasked with solving a maze. The observation space consists of positions and joint angles of the body geometries, while actions correspond to joint torques. Crucially, no information about the maze layout is given, so the agent must learn this through exploration. Reward is 0 unless within a small distance ϵ of the goal, in which case it is 1. Demonstrations from the dataset consist of a non-RL agent navigating between random start and end points within the maze. In particular, the demonstrations are highly suboptimal, often crashing into walls, flipping over, and getting stuck.

Kitchen (Fig. 7(c)) is a task where a Franka Panda arm is tasked with performing a set sequence of 4 subtasks in a mock kitchen environment. Example subtasks might be moving a kettle between burners, turning on the stove, or opening the microwave. Observations consist of position and joint angles of the arm, as well as positions of key objects to be manipulated, and actions are joint torques. Once again, no information about the layout is given to the agent and must be learned through exploration. Rewards are 0 unless the correct subtask is completed in the correct order, which yields a reward of 1. The 4 subtasks must be completed, so there is a maximum reward of 4 available. Demonstrations are collected by humans using a VR interface, and consist of near-perfect executions of different sequences of 4 subtasks from the final subtask sequence.

CoinRun (Fig. 7(d)) is a procedurally-generated platforming game intended to mimic classic games that involves traversing obstacles and avoiding enemies in order to reach a final goal. Each level has a different layout and visual style, designed by humans, in order to require more general recognition from the policy. Observations consist of a 64×64 visual observation of the scene, centered on the agent, with velocity information painted into the upper-left corner. Actions are discrete and consist of moving, jumping, and staying still. Reward is 0 until the final goal for a level is reached, in which case it is 10. For RL, we select a fixed subset of 10 "hard" levels in sequence for an agent to complete, to mimic classic games, so the maximum possible reward is 100. Demonstration data is collected by us through playing around 100 "easy" levels with different layout and visual style than the eventual levels we perform RL on.

E.2 Model

For the model, we choose a 4-layer MLP with 256 hidden units in each layer. We use the default initialization in Stable Baselines 3 [Raffin et al., 2021].

E.3 Optimization

For our RL agent, we use SAC-discrete [Christodoulou, 2019]. Both critics as well as the policy are optimized with Adam with a learning rate of $3e-4$. Replay buffer size is set to the standard 1 million transitions. We update both critics and the policy every step of environment interaction and sample uniformly from the replay buffer to do so. Unlike Christodoulou [2019], we follow a similar convention to Haarnoja et al. [2018b] and automatically optimize α. We choose a target entropy of $-\log|\mathcal{V}|$, except for CoinRun domains, where we use $\frac{1}{2}\cdot\log|\mathcal{V}|$. A negative target entropy may not make sense for a discrete distribution, but we found that any other choice led to extremely unstable optimization due to runaway Q estimates. This hints that SAC may not be well-adjusted to discrete-action sparse-reward domains, as argued by Zhou et al. [2022].

For AntMaze we train for 10 million steps, for Kitchen we train for 2 million, and for CoinRun we train for $500,000$ or til policy divergence. All numbers come from 5 random seeds of training, evaluated over 100 rollouts of the deterministic policy. To avoid biasing numbers, we simply report the final average deterministic performance of the policy, even in cases when performance is better earlier in training.

E.4 Skill-extraction hyperparameters

For AntMazes we choose defaults of $k = 2 \cdot d_{\text{act}}$, $N_{\text{max}} = 128$ and $N_{\text{min}} = 16$. For Kitchen we choose defaults of $k = 2 \cdot d_{\text{act}}$, $N_{\text{max}} = 256$ and $N_{\text{min}} = 16$. For CoinRun there is no need for discretization, so we only choose $N_{\text{max}} = 64$ and $N_{\text{min}} = 16$. These defaults are chosen to approximately match the length 10 skills of SSP, as the choice of k and N_{max} will directly influence the length of discovered skills.

E.5 Implementation

Code was implemented in Python using PyTorch [Paszke et al., 2019] for deep learning, Stable Baselines 3 [Raffin et al., 2021] for RL, and Weights & Biases [Biewald, 2020] for logging.

E.6 Computational Requirements

All experiments were performed on an internal cluster with access to around 100 Nvidia 2080 Ti (or more capable) GPUs. Each single run fits in around 2 GB of GPU memory on a single machine. On AntMaze, training for our method typically takes around 10 hours for a single run, while SSP [Pertsch et al., 2021] takes 12 hours and SFP [Bagatella et al., 2022] takes over a week. In particular, this highlights exactly how poor the scaling can be for methods that call a large model at every transition. More precise information is available in Table 3 (main paper).

F Notes on Reproducibility

One important note to draw from this work is that the results are not always stable. Such inconsistency goes beyond our work alone: the disagreement of dense-reward offline RL [Fu et al., 2020, Emmons et al., 2021, Janner et al., 2021, Wang et al., 2022] numbers; the failure to reproduce SSP baseline results Table 1; and large standard deviations and unclear trends across Tables 1, 6, 7, and 8. In our case, there are a few sources of nondeterminism. We use Scikit-learn [Pedregosa et al., 2011] for our k-means implementation, which yields slightly different results depending on the CPU even with the same seed, which then leads to slightly different skills in the downstream merging process (though they are largely of the same categories). In addition, the library we use for RL, Stable Baselines 3 [Raffin et al., 2021], has subroutines that cannot be controlled on the GPU. Finally, we often observe collapse of the policy during training, which is not an unfamiliar issue in RL. This could be due to the design of SAC [Haarnoja et al., 2018b], which may not easily adapt to the discrete or sparse-reward setting [Zhou et al., 2022], leading to further instability. All the above suggests that five random seeds is not enough to quantify performance [Henderson et al., 2018], however running more samples incurs a significant computational burden, which is not a substantial issue for our method, but is particularly burdensome for baselines. Still, results on exploration in Section 4.2 give us confidence that our modification is working as desired, and we hope that a method like ours may lead to stronger and faster sparse-reward RL in the future.

G Data Quantity

To see how our method performs under limited quantities of data, we subsample the trajectory datasets before generating subwords. We see in Table 10 that less data does not always correlate with worse performance, though the results are mixed as to what is the best setting. Such a result is due to the fact that our subword extraction method only merges the skill that moves "farthest," thus the amount of distracting data is not a core issue, but rather the existence of good skills within that data.

Table 10: Experiments across domains for our method when data is subsampled, by percentage of the original dataset. We see that performance is rather uncorrelated with dataset percentage, which is a result of our subword extraction pipeline.

Task	10%	25%	50%	100%
`antmaze-medium-diverse`	$0.99_{\pm 0.02}$	$0.20_{\pm 0.45}$	$0.80_{\pm 0.45}$	$0.40_{\pm 0.55}$
`antmaze-large-diverse`	0.0	0.0	0.0	$0.34_{\pm 0.46}$
`kitchen-mixed`	$0.20_{\pm 0.04}$	0.0	$0.20_{\pm 0.04}$	$0.72_{\pm 0.40}$
`CoinRun`	$3.44_{\pm 1.40}$	$3.40_{\pm 1.73}$	$2.72_{\pm 2.22}$	$2.90_{\pm 2.90}$

H Effect of Discretization In Locomotion

As mentioned in our Limitations, discretization may remove resolution from the action space that could be useful, in particular for fine-grained manipulation or fast-locomotion tasks. To study this limitation, we investigate the effect of varying the discretization level on the Hopper locomotion task from D4RL [Fu et al., 2020]. We use SaS-freq with $N_{\text{min}} = 32$, $N_{\text{max}} = 128$, training 5 seeds for 3 million steps each.

In Table 11, we see that the conclusions are quite straightforward. More discretization hurts performance, where higher k recovers more of the original action space as smaller regions are clustered together. For simplicity in our sparse-reward results, we used a relatively small number of clusters ($2 \cdot d_{\text{act}}$), but there is no reason why a larger number could not be used in domains that require it.

Table 11: Experiments on the `hopper-expert` domain for varying number of cluster k. Coarser discretization is worse.

k	SaS-freq Reward
12	$2813.3_{\pm 104.4}$
32	$3182.6_{\pm 335.4}$
64	$3248.8_{\pm 137.8}$

I Effect of Data Quality

To see how our method performs under different kinds of data quality, we study SaS-freq on the Hopper task from D4RL [Fu et al., 2020]. This is because, unlike sparse-reward tasks considered in the rest of the paper, Hopper provides a clear delineation of demonstration quality: `random` for transitions from a random policy, `medium` for transitions from a policy partway through training, and `expert` for transitions from a policy at the end of training. We set $k = 12$, $N_{\text{min}} = 32$, $N_{\text{max}} = 128$ and train 5 seeds for 3 million steps.

From Table 12, expert demonstrations provide the best skills, but surprisingly random demonstrations are much more competitive than skills from a medium policy. On further inspection, this is because medium demonstrations contain long segments of the policy standing, which it learns before walking quickly, so the skills discovered primarily relate to standing. In the case of random demonstrations, the skills are quite short in length, so through RL the policy can learn to recombine them. For expert demonstrations this is similar, but the skills are of higher quality.

Table 12: Experiments on the Hopper domain for varying data quality. Random demonstrations outperform medium demonstrations as the skills extracted are much shorter for equivalent hyperparameters, so during RL the policy learns to recombine them.

Task	SaS-freq Reward
`hopper-random`	$2607.3_{\pm 122.0}$
`hopper-medium`	$980.2_{\pm 2.0}$
`hopper-expert`	$2916.1_{\pm 129.3}$

J Q-value Collapse

Here we provide visualizations of the Q-function during RL for one seed of SaS-dist on `antmaze-umaze` that shows good exploration, but at the end of training achieves no reward. We see in Figure 8 that initially Q-estimates are highest on the frontier, but as training progresses, Q-estimates equalize and drive the policy to uniform behavior, which eventually ruins exploration. Combatting such collapse is a large priority in the future for making exploration much more stable.

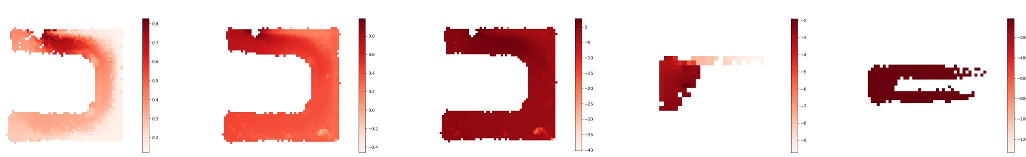

(a) 1m (b) 2m (c) 5m (d) 9m (e) 10m

Figure 8: Q-value for locations in the replay buffer during RL for a seed where optimization collapses. Initially Q-values are aligned with the task, but as optimization progresses, Q-values equalize, which leads to collapse to a random policy.